Research Article

Characteristics of Membranes Derived from Pineapple Biowaste: The Effect of Nanoclay Addition

Nanda Lidya Cinta Aulia Sari and Aminnudin Aminnudin
Department of Mechanical and Industrial Engineering, State University of Malang, Indonesia

Heru Suryanto*
Center for Science and Engineering (PSR), LPPM, State University of Malang, Indonesia

Joseph Selvi Binoj
Institute of Mechanical Engineering, Saveetha School of Engineering, Saveetha Institute of Medical and Technical Sciences (SIMATS), Saveetha University, Chennai, India

Brailson Mansingh Bright
Department of Mechanical Engineering, Sri Ramakrishna Engineering College, Tamilnadu, India

Gaguk Jatisukamto
Department of Mechanical Engineering, University of Jember, East Java, Indonesia

Husni Wahyu Wijaya
Department of Chemistry, State University of Malang, Indonesia

Azlin Fazlina Osman
Faculty of Chemical Engineering Technology, Universiti Malaysia Perlis, Malaysia

Uun Yanuhar
Department of Aquatic Resources Management, Brawijaya University, Indonesia

* Corresponding author. E-mail: heru.suryanto.ft@um.ac.id DOI: 10.14416/j.asep.2025.06.002
Received: 16 February 2025; Revised: 28 March 2025; Accepted: 28 April 2025; Published online: 4 June 2025

Abstract
Indonesia, a major pineapple producer, generates substantial biowaste that can harm the ecosystem. To address this, bacterial cellulose (BC) was produced through microbial fermentation of pineapple peel waste. The study aims to evaluate the properties of BC after it has been reinforced with nanoclay. Methods include cellulose synthesis via fermentation with pineapple biowaste extract, followed by cellulose alkalization, defibrillation, and the synthesis of bacterial cellulose with nanoclay concentrations of 2, 4, 6, and 8 wt.%, which is then dried to form a solid membrane. SEM, XRD, FTIR, tensile testing, antibacterial activity, and porosity analysis were used to characterize the samples. The results show that nanoclay has a considerable influence on the surface morphology of cellulose composites. XRD analysis confirmed that nanoclay incorporation disrupted the BC crystalline structure, reducing crystallinity as nanoclay content increased. Furthermore, nanoclay reduces the membrane's crystallinity index to 75.3% at 8 wt.% nanoclay concentration, FTIR analysis revealed changes in functional groups, indicating strong interactions between BC and nanoclay. Although tensile strength decreased with higher nanoclay content, membrane porosity improved at 6 wt.%, enhancing membrane permeability. Antibacterial testing showed significant inhibition of *E. coli* and *S. aureus*, with the highest activity observed at 8 wt.% nanoclay.

Keywords: Bacterial cellulose, Crystallinity, Membrane, Nanoclay, Pineapple biowaste

1 Introduction

Waste management is a critical challenge affecting sustainable development and environmental quality, particularly in growing urban areas [1]. Indonesia, with a rapidly expanding population and economy, generates about 91,324.49 tons of waste per day tons per day [2] with the majority made up of agricultural waste, sewage sludge, and food waste [3]. Agricultural waste includes all organic waste materials, such as vegetables, fruits, meat, dairy products, poultry, and crops [4]. In 2024, Indonesia produced approximately 2.7 million metric tons of pineapples [5]. Assuming pineapple peels constitute about 13.48% of the fruit's total weight [6]. They generate roughly 363,960.00 metric tons of pineapple peels and require proper management to maximize their societal benefits.

Cellulose is the most abundant biopolymer in the world, widely utilized in many applications [7]. They comprise repetitive anhydrous glucose units that are covalently bound via acetal linkages and include recurring hydroxyl groups. Bacterial cellulose (BC) is a potential form of cellulose synthesized by specific bacterial species consisting of β-1→4 glucan chain assembled by hydrogen bond [8]. BC contributes to its utility in various industries, including healthcare [9], packaging [10], and membrane technology [11].

Membranes are categorized into polymeric and inorganic types depending on their composition [12]. Polymeric membranes are widely preferred due to their affordability, tunable pore sizes, configurational flexibility, and scalability [13]. The incorporation of nanomaterials has led to the development of polymeric nanocomposite membranes with enhanced mechanical strength, thermal stability, and separation efficiency [12], [14]. Among these, nanoclay stands out due to its layered silicate structure, which improves the physical and chemical properties of polymer composites [15]. It enhances mechanical strength, durability, and adsorption capacity, making it valuable for high-performance membrane applications [16].

Despite these advantages, polymer-nanoclay composites face challenges, particularly in achieving uniform nanoclay dispersion, ensuring compatibility, and maintaining scalability. In bacterial cellulose (BC) membranes, nanoclay integration is especially challenging due to agglomeration and variable interactions within the polymer matrix. While BC membranes are well-studied for their biocompatibility, structural integrity, and filtration capabilities [17], the effects of nanoclay on crystallinity, porosity, and antibacterial properties remain insufficiently explored. Overcoming dispersion issues is critical for optimizing nanoclay-enhanced BC membranes [18], [19].

The influence of nanoclay on BC membrane properties remains insufficiently explored, making it challenging to optimize nanoclay content for practical applications. This study aims to develop a bacterial cellulose membrane from pineapple peel waste and evaluate the impact of nanoclay on its characteristics. The membrane's suitability for potential applications is evaluated using characterization techniques such as scanning electron microscopy (SEM), X-ray diffraction (XRD) for crystallinity, Fourier transform infrared spectroscopy (FTIR) for chemical bonding, tensile testing for mechanical properties, and antibacterial testing.

2 Material and Methods

2.1 *Materials*

The pineapple peel waste collected from local sources (region of Malang, East Java, Indonesia) and *Acetobacter xylinum* strains were provided by the Microbiology Laboratory, Muhammadiyah University Malang, Indonesia. The nanoclay was purchased from Sigma-Aldrich, USA.

2.2 *Bacterial cellulose synthesis process*

BC synthesis was conducted according to the previously published procedure using a static batch fermentation which is effective for uniform cellulose formation at the air-liquid interface [8]. The process of cellulose synthesis began by mixing 300 g of pineapple peel waste with 2 L of water using a blender for 10 min at 26,000 rpm to release essential nutrients. The mixture was filtered to obtain pineapple peel extract. 2 L extract was then boiled for 15 min. to eliminate unwanted microbes, and cooled until room temperature for use as the fermentation medium. The fermentation was started by adding 10% of *A. xylinum* into the 1 L extract containing 100 g glucose as the carbon source and 5 g ammonium acid as the nitrogen source, then adjusting the pH at 4.5 using acetic acid solution (purity 99.7%, Smart-Lab, Indonesia) to create optimal growth conditions for *A. xylinum* while minimizing contamination. The fermentation process was conducted under static conditions at 25–30 °C for 10 days, allowing BC to form as a floating pellicle at the air-liquid interface. After 10 days, the BC was harvested and rinsed thoroughly with water until a neutral pH was achieved to remove residual fermentation

components and impurities. This method effectively utilizes pineapple peel waste as a sustainable and cost-efficient substrate for bacterial cellulose production.

2.3 *Bacterial cellulose defibrillation*

Defibrillated BC was produced following previously published methods [20] to break down BC networks into nanoscale fibrils. Fibrillated BC was prepared by adding 600 mL of deionized water (dH_2O) with 6% NaOH solution to facilitate cellulose swelling and partial hydrolysis. 200 g of BC produced from the fermentation process were added into the solution and heated at 90 °C for 2 h to remove residual bacteria, proteins, and other impurities while enhancing fiber separation. The boiled BC was washed at least twice with dH_2O until neutral to ensure the removal of excess alkali. To achieve finer fibrillation, 50 g of BC was mixed with 1 L of dH_2O and then crushed using a blender (Wirastar, Indonesia) for 5 min, 3 times to break down larger cellulose aggregates. The slurry was then further processed using a high-pressure homogenizer (AH-100D, Berkeley Scientific, China) for five cycles at 150 bar, which exerted intense shear forces to separate BC fibers into nano-sized fibrils. Finally, the fibrillated BC was filtered to remove any remaining large particles and prepared for further processing.

2.4 *Synthesis of bacterial cellulose membrane nanocomposite*

The membrane fabrication process involved incorporating nanoclay into the bacterial cellulose (BC) matrix through a dispersing and casting method. This step includes the preparation of BC in the procedures of alkalization and defibrillation (section 2.3) to improve fiber dispersion. The process began by dispersing 10 g of fibrillated BC in 100 mL of dH_2O and stirring for 30 min. to ensure uniform distribution of cellulose fibrils. Simultaneously, the nanoclay at concentrations of 2, 4, 6, and 8 wt.% was separately dissolved into 100 mL of dH_2O for each concentration, followed by stirring for 30 minutes to minimize agglomeration and achieve homogeneous dispersion. To further break down nanoclay agglomerates and enhance their interaction with BC, the nanoclay mixture was subjected to ultrasonic treatment using a sonicator (400 W, 20 kHz, Ningbo Lawson Smarttech, China) for two cycles of 30 min each. This high-energy sonication process helps to exfoliate nanoclay layers, increasing surface area and improving dispersion within the BC matrix. After sonication, the nanoclay suspension was combined with the fibrillated BC solution, poured into a mold, and dried in an oven at 50 °C for approximately 20 h. The slow drying process ensured uniform film formation and minimized defects, leading to the development of a stable BC/nanoclay nanocomposite with enhanced structural integrity.

2.5 *Characterization*

The structural and morphological characteristics of the BC/nanoclay membrane were analyzed to evaluate its surface features and crystallinity. The BC/Nanoclay membrane's shape and surface morphology were examined using Scanning Electron Microscopy-SEM (FEI Inspect S50, Japan) to observe the distribution of nanoclay within the BC matrix. Before SEM inspection, the membrane's surface was coated with a thin layer of gold around 10 nm thick using a film coater to enhance conductivity and improve imaging quality. The crystallinity of the BC/nanoclay membrane was determined by X-ray Diffraction (XRD, PanAnalytical X'pert pro, USA) for samples with dimensions of 10 x 10 mm^2. Scanning was performed utilizing diffraction angles ranging from 10° to 90°, CuKα wavelength (λ) 1.54, 30 mA, and 40 kV. Crystalline index (CI) and crystallite size (CS) was calculated using Equations (1) and (2), respectively, to quantify the degree of crystallinity and the average size of crystalline domains, helping to determine the impact of nanoclay reinforcement on the BC matrix.

$$CI = \frac{I_{22} - I_{18}}{I_{22}} x\ 100\% \quad (1)$$

$$CS = \frac{K\,\lambda}{\beta cos\theta} \quad (2)$$

The BC/nanoclay membrane was further characterized to evaluate its chemical composition, mechanical properties, and porosity. The functional group analysis was carried out using Fourier Transform Infrared (FTIR) spectroscopy (Prestige-21 type instrument, Shimadzu, Japan), which scanned from 400 to 4000 cm^{-1}, to provide insight into molecular interactions between BC and nanoclay, allowing the identification of characteristic absorption peaks corresponding to cellulose, nanoclay, and possible functional modifications. The mechanical strength testing followed the ASTM D638-V standard. The test was repeated three times with a pulling rate of 3.5 mm/min, and the average value was calculated

to ensure reliability. The samples were formed according to ASTM D638-V and inserted between tensile testing machine grips. The porosity of the membrane was measured using BET (Brunauer-Emmett-Teller, Micromeristic Instrument, USA) method. The test used nitrogen gas as the adsorbate medium. Prior to examination, the membrane samples were degassed at 105 °C for 4 h to remove any residual moisture or contaminants that could interfere with adsorption measurements.

2.6 *Antibacterial activity*

The evaluation of the antibacterial activity of the BC/nanoclay membrane was conducted using two different bacteria: *Staphylococcus aureus* (Gram-positive) and *Escherichia coli* (Gram-negative) to determine its effectiveness in inhibiting bacterial growth. The agar disk diffusion method was employed, where membrane samples were prepared in circular discs of 5 mm diameter. BC control membrane, tested alongside the antibiotic chloramphenicol, served as the positive control to compare antibacterial effectiveness. The BC membranes containing nanoclay with concentrations of 0, 2, 4, 6, and 8 wt.% was designated as Samples I, II, III, IV, and V, respectively. After the incubation process, the inhibition zones around each sample were measured. The size of these zones revealed the antibacterial activity of each membrane. Larger inhibition zones indicated stronger antibacterial properties, demonstrating the impact of nanoclay incorporation on bacterial suppression.

3 Result and Discussion

3.1 *Analysis of bacterial cellulose nanocomposite morphology*

BC/nanoclay morphology was observed under SEM with results as shown in Figure 1, which reveals distinct differences across various nanoclay concentrations. Figure 1(a) shows the BC membrane without any reinforcement. The pure BC membrane exhibits a smooth and uniform surface with a well-organized fibrous network. At 2 wt.% nanoclay (Figure 1(b)), the clay particles are visible throughout the nanocomposite as small aggregates on the surface, maintaining structural homogeneity. (Figure 1(c)). At 4 wt.% nanoclay (Figure 1(c)), small clusters of nanoclay begin to form, and agglomeration becomes visible, leading to irregularities in the BC structure, and reduced uniformity and slight distortion of the fibrous structure. A more significant change is observed at 6 wt.% nanoclay (Figure 1(d)), where nanoclay agglomeration becomes prominent, creating a rougher surface and increasing particle inclusions, thereby disrupting the BC network. Nanoclay leads to excessive clustering, causing poor nanoclay dispersion and highly distorted BC fibrils. The most severe structural disruption occurs at 8 wt.% nanoclay (Figure 1(e)), where strong van der Waals forces lead to excessive clustering, causing poor nanoclay dispersion and highly distorted BC fibrils. This progression suggests that lower nanoclay concentrations (2–4 wt.%) maintain uniform dispersion with minimal impact on BC structure. Whereas higher concentrations (6–8 wt.%) result in significant aggregation, which can affect mechanical strength, crystallinity, and overall membrane performance.

Different morphology is caused by nanoclay agglomeration due to van der Waals forces of nanoclay [21]. These forces cause the particles to interact and cluster together rather than uniform dispersion, which affects the mechanical and structural properties of the nanocomposite. Agglomeration also occurred due to no surface modification using nanoclay. Modification exchanges the inorganic cations naturally present in the clay with modifiers such as alkylammonium, or phosphonium ions, that expand the interlayer spacing [18] to improve chemical compatibility in the BC matrix. Another process identified is insufficient sonication causes the nanoclay to not be completely broken down and remain in the form of agglomerates. On the other hand, excessive sonication can collapse the BC structure [22], which interferes with the dispersion of nanoclay.

The BC membrane exhibits reduced crystallinity after the homogenization process, resulting in a more evenly dispersed nanoclay. The SEM analysis also highlights that the nanoclay reinforcement alters the surface morphology, indicating enhanced interfacial bonding between the BC matrix and nanoclay.

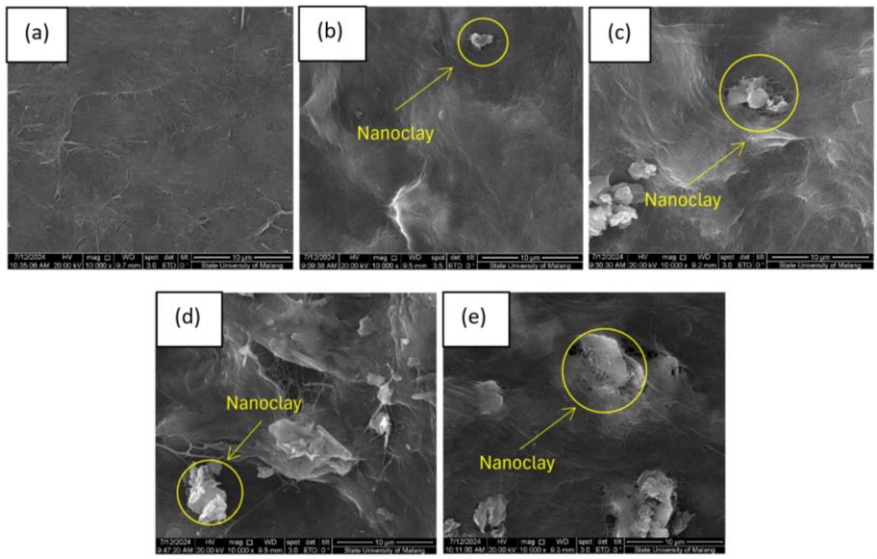

Figure 1: Morphology of BC membrane (a) without addition, the addition of nanoclay: (b) 2 wt.%, (c) 4 wt.%, (d) 6 wt.%, and (e) 8 wt.%.

3.2 *Crystallinity analysis of bacterial cellulose nanocomposite*

The crystallinity of BC was affected by the addition of nanoclay. The result of crystalline analysis is depicted in Figure 2 and Table 1.

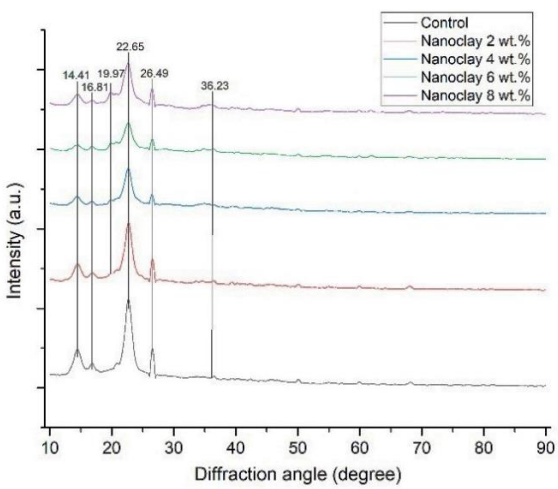

Figure 2: Diffraction pattern of BC membrane with nanoclay reinforcement.

Diffraction peaks of the membrane observed at ~14°, 16°, 19°, 22°, 26°, and 36°. The peaks ~15°, ~16°, and ~22° is corresponding to the cellulose I_β structure [23]. Nanoclay insertion resulted in additional peaks at ~19° and 36°. The emergence of an XRD peak of 26.49° in BC membrane is atypical for standard cellulose structures. This may indicate the formation of additional crystalline phases or the presence of impurities introduced during the pretreatment process using alkali. This phenomenon is also found in banyan aerial root fiber after alkali treatment [24] and also in nanofiber from rubber leaves after bleaching treatment [25].

Membrane control has a CS of 29.08 nm. At low nanoclay concentrations, such as 2 wt.%, a reduction in CS occurs at 9.25 nm. The nanoclay tends to disperse well within the bacterial cellulose (BC) matrix leading to effective intercalation between the cellulose fibrils. Better dispersion disrupts the crystalline order, reducing the CS, and resulting in improved homogeneity of the composite. However, as the concentration of nanoclay increases specifically at 4%, 6%, and 8 wt.% agglomeration of nanoclay particles occurs due to van der Waals forces between the particles, as revealed by SEM analysis (Figure 1). This agglomeration leads to uneven particle distribution within the BC matrix, disrupting the crystalline order and causing fluctuations in CS, which ranged from 8.48 nm to 10.18 nm for the higher concentrations. The 2 wt.% nanoclay concentration likely provides the optimal balance between dispersion (Figure 1(a)) and interfacial interaction with the BC network resulting in better mechanical

strength compared to the other nanoclay concentrations (see Figure 4).

Additionally, the incorporation of nanoclay reduces the CI of the BC membrane, indicating a disruption in the structural order of the crystalline material. CI decreased with the addition of nanoclay from 81.6% (BC control) to 75.3% (8% nanoclay), indicating that nanoclay disrupted the BC crystalline structure. This effect becomes more pronounced with increasing nanoclay concentrations, as the formation of an ideal crystalline structure is hindered by complex interactions with nanoclay particles. Moreover, the higher solution viscosity at higher nanoclay content may obstruct polymer chain intercalation among the clay lamellae, affecting crystallite formation. Tsekova and Stailova (2022) indicate that higher content of nanoclay (10 wt.%) in cellulose acetate makes membranes more amorphous structure but increases their adsorption capacity to dyes [26].

Table 1: Peak in diffraction angle and crystalline properties of BC/nanoclay membrane.

Sample	Peak in Diffraction Angle (°)						CI (%)	CS (nm)
Control	14.49	16.87	-	22.69	26.65	-	81.6%	29.08
BC/Nanoclay 2 wt.%	14.49	16.91	19.97	22.69	26.57	36.41	79.8%	9.25
BC/Nanoclay 4 wt.%	14.41	16.83	19.89	22.67	26.45	36.39	76.6%	10.18
BC/Nanoclay 6 wt.%	14.47	16.77	19.89	22.65	26.51	36.27	76.3%	8.48
BC/Nanoclay 8 wt.%	14.41	16.89	19.87	22.65	26.49	36.23	75.3%	10.18

The CS initially decreased at 2% (9.25 nm) but fluctuated at higher concentrations due to nanoclay aggregation. As the nanoclay concentration increases up to 6 wt.%, the CS decreases, indicating enhanced intercalation or partial exfoliation of the nanoclay layers. However, at 4 wt.% and 8 wt.%, the CS stabilizes around 10.18 nm, suggesting partial intercalation with reduced exfoliation. This trend implies that higher nanoclay concentrations initially promote structural disruption and intercalation, but beyond a certain point, the structure stabilizes, resulting in minimal changes in CS.

The observed difference in crystalline properties after adding various nanoclay content can be attributed to multiple factors, including the dispersion efficiency [27], interaction forces between the nanoclay and the polymer matrix [28], and the degree of exfoliation [29] or agglomeration [30]. At lower concentrations (2 wt.%), the nanoclay is more uniformly distributed, leading to better interaction with the cellulose matrix and a greater reduction in CS. However, at higher concentrations, agglomeration effects dominate, reducing the effectiveness of intercalation and affecting the overall crystalline structure.

The significant reduction in CS observed at lower nanoclay concentrations suggests potential applications in nanocomposite membrane design, where finer crystalline structures may enhance specific functionalities. For example, membranes with smaller crystallites could exhibit improved flexibility, better adsorption properties, or enhanced interaction with target molecules in filtration applications. Future studies should explore optimizing nanoclay dispersion techniques, such as the surface modification or ultrasonic treatment, to maintain a fine crystalline structure while minimizing aggregation effects. Additionally, investigating the relationship between CS and mechanical or permeability properties could provide deeper insights into tailoring bacterial cellulose nanocomposites for advanced applications.

3.3 *Functional group analysis*

Analysis of the functional group of BC/nanoclay membrane using FTIR is shown in Figure 3. The O–H stretching vibration observed around 3200–3600 cm^{-1} is attributed to the extensive hydrogen bonding network in bacterial nanocellulose, indicating the presence of hydroxyl groups that contribute to its hydrophilic nature [31]. The lower transmittance of the BC membrane after adding nanoclay indicates that the membrane has more hydrophilic properties. The C–H stretching peak near 2800–2900 cm^{-1} corresponds to the aliphatic –CH and $–CH_2$ groups in cellulose, reflecting the polysaccharide structure of bacterial cellulose [32]. The presence of nanoclay disrupts the cellulose matrix, causing shifts in molecular alignment. This disruption modifies the dipole moment of the C–H bond, reducing IR absorption efficiency and thus lowering transmittance. The peak at 1730–1740 cm^{-1} represents C=O stretching, which may originate from acetyl or carboxyl groups from the pineapple peel-derived cellulose or oxidation during processing [33]. Nanoclays contain functionalized surfaces (e.g., hydroxyl groups (silanols and aluminols), carboxyl, or amine groups) [34] that interact with the C=O groups in the cellulose matrix. These interactions modify electron density around the C=O bond, affecting its IR

absorption. The C–H bending vibrations observed in the 1250–1450 cm^{-1} range are associated with cellulose deformation [35]. Lastly, new peaks are present in wavenumber in the range 900–1100 cm^{-1} that indicate the characteristic Si–O–Si stretching, confirming the presence of nanoclay, indicating its dispersion within the nanocomposite matrix [36].

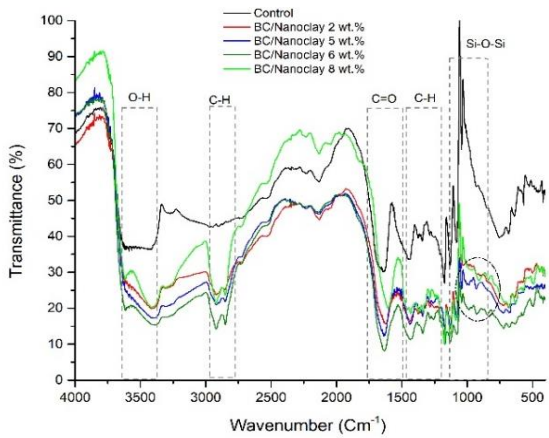

Figure 3: FTIR analysis of BC membrane reinforced by nanoclay.

3.4 *Mechanical properties*

Figure 4 shows the results of the tensile test of BC with the addition of various concentrations of nanoclay.

The tensile strength of the material decreases with the addition of nanoclay compared to the control, which shows the highest tensile strength at 26.76 MPa. 2 wt.% nanoclay showed the least reduction in tensile strength compared to the BC pure. The tensile strength drops to 22.22 MPa, indicating a reduction in the material's mechanical performance. As nanoclay concentration increases to 4 wt.%, the tensile strength continues to decline sharply to 13.85 MPa, possibly due to particle agglomeration or uneven dispersion in the matrix and possible weak points. However, as the nanoclay concentration reaches 6 wt.%, the tensile strength slightly improves to 14.15 MPa, indicating that at higher concentrations, the dispersion of nanoclay improved. At 8 wt.%, the tensile strength further increases to 15.37 MPa, which suggests that higher nanoclay content might enhance the material's structure. 8 wt.% nanoclay slightly improved over 6% but remained significantly weaker than the control.

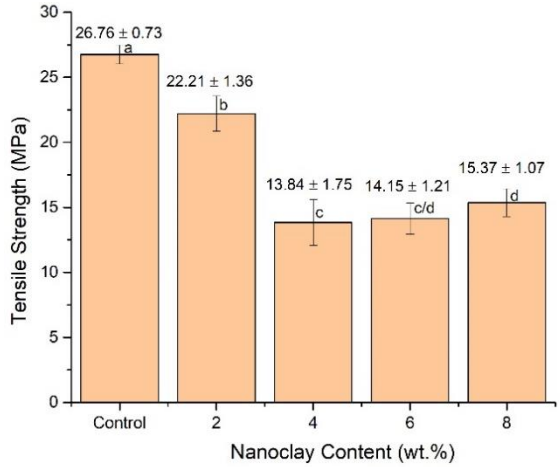

Figure 4: Tensile strength of BC membrane reinforced by nanoclay. Note: the same notation (a) to (d) are not significantly different (n=3, *p*-value > 0.05).

The addition of nanoclay results in a lower tensile strength compare to the control. The relationship between nanoclay concentration and tensile strength follows a non-linear trend. At 2% nanoclay, the tensile strength shows the least reduction compared to the control, suggesting that at this level, the nanoclay is well-dispersed, reinforcing the bacterial cellulose (BC) matrix (Figure 1(a)) without significantly disrupting its polymer network. However, as the nanoclay concentration increases beyond 2%, aggregation effects become more dominant (Figure 1(c) to (e)), leading to potential weak points in the structure and a decline in tensile properties. This aligns with the CI of 79.8% at 2% nanoclay, which indicates a moderate disruption in crystalline order while maintaining structural integrity. However, as the nanoclay concentration increases beyond 2%, aggregation effects become more dominant, leading to potential weak points in the structure and a decline in tensile properties. The CI drops further to 76.6% at 4%, 76.3% at 6%, and 75.3% at 8%, confirming that higher nanoclay concentrations increasingly interfere with the crystalline structure.

Interestingly, a higher nanoclay percentage does not necessarily result in the lowest tensile strength. While excessive nanoclay can lead to agglomeration and structural inhomogeneity, certain concentrations—such as 6% or 8%—may still exhibit improved interfacial bonding compared to intermediate levels like 4%. This is because, at specific concentrations, the dispersion and interaction between nanoclay and BC fibers may still provide some reinforcement. Therefore, optimizing nanoclay content is crucial to balancing mechanical reinforcement with structural integrity,

rather than assuming that increasing nanoclay always weakens the material. This variation may be caused by nanoclay's influence on the structural integrity of the material, including factors such as particle dispersion, matrix interaction, and potential agglomeration at different concentrations [37], [38]. The HPH process also contributes to the structure of the BC membrane, including changes in the fiber network, resulting in the influence of the tensile strength [39].

Figure 5 demonstrates how the change in composition affects Young's Modulus. Young's Modulus is a measure of the stiffness of the material. The control has the highest Young's Modulus at 36.77 MPa. By increasing the composition up to 2%, Young's Modulus falls notably to 16.66 MPa, showing an apparent decline in stiffness [40]. This decline continues at 4%, where the modulus further decreases to 8.63 MPa, indicating the material has become even more flexible. However, as the composition increases to 6%, there is a slight recovery in stiffness, with a modulus of 12.16 MPa. Finally, at 8%, Young's Modulus rises modestly to 15.99 MPa, yet it remains significantly lower than the control. Overall, the trend shows that increasing the composition initially leads to a decrease in Young's Modulus, though beyond 4 wt.% nanoclay concentration, the material regains some stiffness.

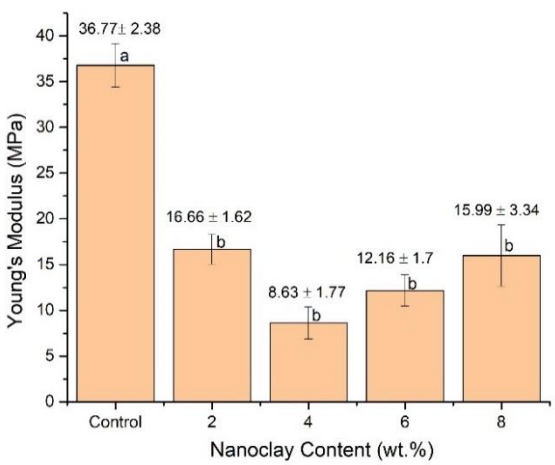

Figure 5: Young's modulus of BC membrane reinforced by nanoclay. Note: the same notation (a) and (b) is not significantly different (n=3, *p*-value > 0.05).

One-way ANOVA revealed that nanoclay addition significantly affected both the tensile strength and Young's modulus of the BC membrane (*p*-value < 0.05). While certain nanoclay contents enhanced these properties, they were generally lower than those of the control membrane, likely due to variations in nanoclay dispersion, agglomeration, and matrix interactions. Tukey's test showed that all nanoclay concentrations had significantly different tensile strengths compared to the control (*p*-value < 0.05). However, only the 2 wt.% nanoclay concentration exhibited a significant difference in tensile strength compared to the other concentrations (4, 6, and 8 wt.%) (*p*-value < 0.05). For Young's modulus, Tukey's test indicated that all nanoclay concentrations were significantly different from the control, but variations among nanoclay additions up to 8 wt.% were not statistically significant. The observed fluctuations may be attributed to uneven nanoclay dispersion or localized stress concentrations within the membrane structure. Similar results were shown by Sobahi *et al*., that indicates the addition of 5 wt.% various nanoclay reduce the mechanical properties of cellulose triacetate nanocomposite [41].

In the tensile results, particle agglomeration or poor dispersion in the BC/nanoclay matrix leads to a significant reduction in strength due to several factors. Agglomerated nanoclay particles act as localized stress concentrations [42], acting as weak points that reduce the efficiency of load transfer within the BC structure. Instead of reinforcing the material, these clusters become structural defects that initiate cracks under applied stress. Additionally, poor dispersion cause poor interfacial bonding [43] between nanoclay and BC, preventing effective stress distribution and leading to premature failure. The presence of large nanoclay aggregates also restricts polymer chain mobility, making the BC membrane brittle and less capable of absorbing tensile stress. Furthermore, phase separation and structural inhomogeneity result in regions with excess nanoclay and others with little reinforcement, causing inconsistent mechanical properties across the membrane. As a result, the lack of uniform dispersion disrupts the material's integrity, ultimately lowering tensile strength and making the membrane more prone to fracture under mechanical loading.

3.5 *Antibacterial activity*

The antibacterial activity of BC/nanoclay nanocomposite membrane was evaluated using *E. coli* (Gram-negative) and *S. aureus* (Gram-positive) as test pathogens. The test disk was carefully placed on the inoculated agar medium, where it absorbed moisture, facilitating the diffusion of the antimicrobial agent into the surrounding agar. This process created a concentration gradient of the antibacterial substance, as shown in Figure 6 and the quantitative measurement of halo diameter was summarized in Table 2.

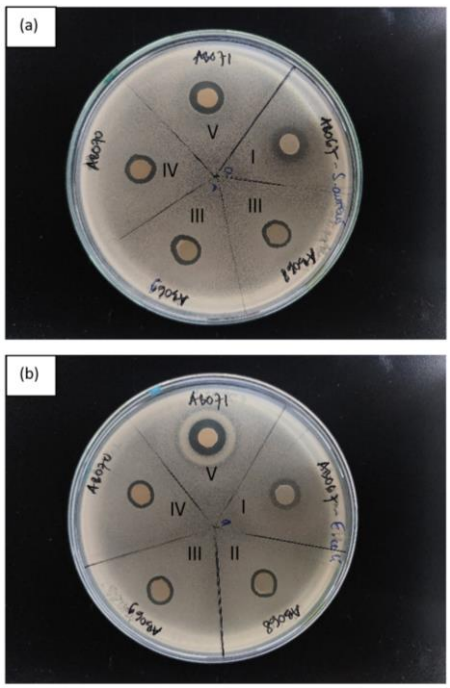

Figure 6: Antibacterial test: (I), BC membrane with nanoclay of 2% (II); 4% (III); 6% (IV); and 8% (V); against (a) *E. coli* and (b) *S. aureus*.

Table 2: Antibacterial activity of nanoclay.

Sample	Diameter Zone (mm)	
	E.coli	***S.aureus***
Positive control	21.85	23.82
BC	6.5 ± 3.2	6.1 ± 3.1
BC/nanoclay 2 wt.%	8.9 ± 0.8	9.0 ± 0.3
BC/nanoclay 4 wt.%	9.3 ± 0.6	9.7 ± 0.3
BC/nanoclay 6 wt.%	9.6 ± 0.1	9.8 ± 0.2
BC/nanoclay 8 wt.%	11.4 ± 0.4	10.3 ± 0.4

A blur zone was observed around the control samples for *E. coli* (Figure 6(a)-I) and *S. aureus* (Figure 6(b)-I), with inhibition zones of 6.5 ± 3.2 mm and 6.1 ± 3.1 mm, respectively. Nanoclay content in the BC membrane exhibited antibacterial activity against both bacterial strains. With 2 wt.% nanoclay, the inhibition zones measured 8.9 ± 0.8 mm (Figure 6(a)-II) for *E. coli* and 9.0 ± 0.3 mm (Figure 6(b)-II) for *S. aureus*. At 4 wt.%, inhibition zones increased to 9.3 ± 0.6 mm (Figure 6(a)-III) and 9.7 ± 0.3 mm (Figure 6(b)-III). Further, nanoclay with 6 wt.% resulted in inhibition zones of 9.6 ± 0.1 mm (Figure 6(a)-IV) and 9.8 ± 0.2 mm (Figure 6(b)-IV). The highest reinforcement level (8 wt.%) showed the largest inhibition zones at 11.4 ± 0.4 mm (Figure 6(a)-V) and 10.3 ± 0.4 mm (Figure 6(b)-V). The inhibition zone diameter increased with higher nanoclay concentrations, indicating enhanced antibacterial activity [36]. However, the BC/nanoclay nanocomposite membrane exhibited lower antibacterial efficacy against *E. coli* and *S. aureus* compared to the chloramphenicol as a positive control, with a diameter zone of 21.85 and 23.82 mm, respectively.

The antibacterial performance of the BC/nanoclay membrane varies depending on the specific microbial group tested. *E. coli* (Gram-negative) and *S. aureus* (Gram-positive) have distinct cell wall structures, which influence their susceptibility to nanoclay-enhanced membranes. *E. coli* possesses an outer membrane rich in lipopolysaccharides, which acts as a barrier against antimicrobial agents, potentially reducing the direct interaction of nanoclay with bacterial cells. This can result in a lower antibacterial effect at the same nanoclay concentration compared to Gram-positive bacteria. In contrast, *S. aureus*, with its thicker peptidoglycan layer but lack of an outer membrane, is more exposed to direct interaction with nanoclay, making it more susceptible to disruption. Additionally, nanoclay exerts antibacterial effects through multiple mechanisms, such as physical disruption of the bacterial membrane integrity [44]. All of which vary in efficiency depending on bacterial structure. The observed increase in inhibition zones (from 6.5 mm in the BC membrane to 11.4 mm at 8% nanoclay for *E. coli*, and from 6.1 mm to 10.3 mm for *S. aureus*) highlights the impact of nanoclay content on bacterial suppression. This suggests that nanoclay is more effective against Gram-positive bacteria due to easier penetration and stronger interactions, whereas *E. coli*'s outer membrane limits direct antimicrobial activity. Thus, *S. aureus* exhibits a larger inhibition zone because nanoclay can more efficiently interact with and disrupt its cell wall compared to *E. coli*, which has an additional protective barrier.

This finding aligns with Vazifeh *et al*., who reported that incorporating 1% nanoclay into chitosan film enhanced antibacterial activity against *E. coli* and *S. aureus*, while higher nanoclay concentrations reduced its effectiveness [45]. Similarly, Mohsen *et al*., demonstrated that increasing clay nanoparticle content in a PVA matrix improved *E. coli* inhibition [46]. In a polyurethane, 5 wt.% modified clay achieved a 98.5% killing efficiency against *E. coli* and 99.9% against *S. aureus* [47].

3.6 *Porosity analysis*

Figure 7 presents the effect of nanoclay concentration on the pore size distribution of BC/Nanoclay membranes. The nitrogen adsorption-desorption analysis was conducted to assess the mesoporous structure of these membranes, which shows how nanoclay incorporation affects pore characteristics. The porosity analysis indicates that as nanoclay content increases (2, 4, 6, and 8 wt.%), pore size gradually expands, reaching an optimum at 6 wt.% nanoclay concentration. This trend suggests that nanoclay additions enhance the formation of interconnected mesopores, providing a larger surface area for adsorption. However, at 8 wt.% nanoclay, a slight decrease in pore size is observed, which could result from the agglomeration of nanoclay particles. This agglomeration reduces effective porosity by blocking some of the pores, thus decreasing the average pore diameter and limiting accessible surface area [48]. This phenomenon demonstrates that nanoclay enhances pore distribution [49].

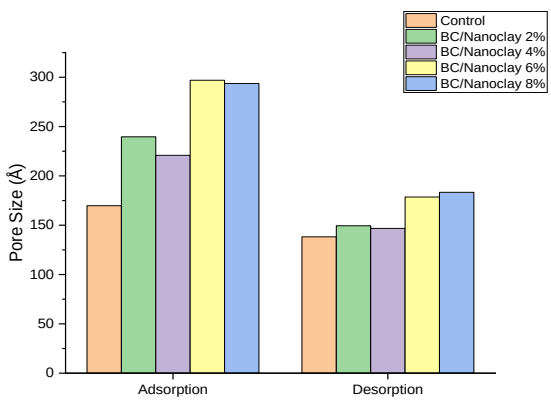

Figure 7: Adsorption-desorption isotherm graph of BC/Nanoclay.

The pore size distribution generated from adsorption data shows a shift toward larger pores when nanoclay concentrations rise to 6 wt.%, resulting in a well-developed mesoporous network that is particularly useful for filtering and adsorption applications. The rise in average pore diameter at this concentration suggests a more open pore structure, which allows for more adsorptive capacity. This is due to nanoclay particles acting as spacers between BNC fibrils, which creates new routes and improves overall pore connectivity.

4 Conclusions

The influence of nanoclay content on BC-based nanocomposite membranes was investigated using SEM, XRD, FTIR, tensile testing, and antibacterial tests. Nanoclay reinforcement resulted in membrane agglomeration and inclusions. Nanoclay incorporation modified the crystallinity of the BC membrane, introducing new diffraction peaks and reducing CS, particularly at 2 wt.% due to enhanced dispersion and intercalation. However, at higher concentrations, nanoclay agglomeration disrupted the crystalline structure, stabilizing CS. CI dropped from 81.6% (control) to 75.3% (8 wt.% nanoclay). FTIR analysis confirmed the successful incorporation of nanoclay into the BC membrane, evidenced by Si–O–Si stretching vibrations. Tensile strength decreased from 26.7 MPa (control) to 15.37 MPa (8 wt.% nanoclay). Antibacterial tests revealed lower activity than chloramphenicol, the positive control, but considerable improvement with increasing nanoclay. While 6% nanoclay provided the highest porosity, it was not optimal across all parameters. Notably, 8% nanoclay demonstrated the strongest antibacterial activity, with inhibition zones of 11.4 mm for *E. coli* and 10.3 mm for *S. aureus*, highlighting its microbial suppression effectiveness. The results suggest that the ideal nanoclay concentration depends on the desired properties 6% for permeability, 2% for mechanical strength, and 8% for antibacterial performance. Future studies should focus on enhancing nanoclay dispersion and balancing these properties to develop a versatile membrane for filtration, biomedical, and antimicrobial applications.

Acknowledgments

Gratitude is extended to LPPM Universitas Negeri Malang for supporting this research through the Penelitian Unggulan Pusat scheme under contract number 4.4.796/UN32.14.1/LT/2024.

Author Contributions

N.S.: investigation, drafting, writing an original; H.S.: funding acquisition, research design, methodology, reviewing and editing; A.A.: research design, data analysis; J.S.B.: data analysis, reviewing and editing; B.M.B: data analysis, reviewing and editing; G.J.: data curation, project administration. H.W.W.: A.F.O.: data analysis, reviewing, and editing; U.Y.: data analysis, reviewing, and editing. All authors have read and agreed to the published version of the manuscript.

Conflicts of Interest

The authors declare no conflict of interest.

References

[1] K. Zaman, M. Malik, U. Awan, W. Handayani, M. K. Jabor, and M. Asif, "Environmental effects of bio-waste recycling on industrial circular economy and eco-sustainability," *Recycling*, vol. 7, no. 4, 2022, doi: 10.3390/recycling7040060.

[2] N. Putu and W. Romianingsih, "Waste to energy in Indonesia: Opportunities and challenges," *Journal of Sustainability, Society and Eco-Welfare*, vol. 1, no. 1, pp. 60–69, 2023, doi: 10.61511/jssew.v1i1.

[3] M. Xu, M. Yang, H. Sun, M. Gao, Q. Wang, and C. Wu, "Bioconversion of biowaste into renewable energy and resources: A sustainable strategy," *Environment Research*, vol. 214, p. 113929, 2022, doi: 10.1016/j.envres.2022.113929.

[4] P. Pangsri, T. Wuttipornpun, and W. Songserm, "Mannanase and cellulase enzyme production from the agricultural wastes by the *bacillus subtilis* P2-5 strain," *Applied Science and Engineering Progress*, vol. 14, no. 3, pp. 425–434, Jul. 2021, doi: 10.14416/j.asep.2020.05.002.

[5] M. Siahaan. "Indonesia: Production of pineapple 2024." statista.com. https://www.statista.com/statistics/706517/production-of-pineapple-in-indonesia/ (accessed Mar. 18, 2025).

[6] Y. S. K. Dewi and C. J. K. Simamora, "Pineapple (*Ananas comosus* [L.] Merr.) Cv. queen peel herbal tea with a variety of drying temperatures: bioactive compounds, antioxidant activity and antimicrobial activity," *Food Research*, vol. 7, no. 4, pp. 344–351, Aug. 2023, doi: 10.26656/fr.2017.7(4).005.

[7] N. Kongkum, V. Phakeenuya, and S. Kongruang, "Optimization of microcrystalline cellulose production from Brewer's Spent grain by acid hydrolysis," *Applied Science and Engineering Progress*, vol. 18, no. 2, p. 7624, 2025, doi: 10.14416/j.asep.2024.11.002.

[8] U. Yanuhar, H. Suryanto, I. K. Ningrum, and A. Aminnudin, "Effect of titanium dioxide nanoparticle on properties of nanocomposite membrane made of bacterial cellulose," *Journal of Natural Fibers*, vol. 19, no. 16, pp. 13914–13927, 2022, doi: 10.1080/15440478.2022.2112797.

[9] A. Pandey, M. K. Singh, and A. Singh, "Bacterial cellulose: A smart biomaterial for biomedical applications," *Journal of Material Research*, vol. 39, no. 1, pp. 2–18, 2024, doi: 10.1557/s43578-023-01116-4.

[10] P. Cazón and M. Vázquez, "Bacterial cellulose as a biodegradable food packaging material: A review," *Food Hydrocolloid*, vol.113, p. 106530, 2021, doi: 10.1016/j.foodhyd.2020.106530.

[11] T. Mahsuli, A. Larasati, A. Aminnudin, and J. Maulana, "Effect of the homogenization process on titanium oxide-reinforced nanocellulose composite membranes," *Journal of Mechanical Engineering Science and Technology (JMEST)*, vol. 7, no. 2, pp. 137–146, Nov. 2023, doi: 10.17977/um016v7i22023p137.

[12] N. F. Al Harby, M. El-Batouti, and M. M. Elewa, "Prospects of Polymeric nanocomposite membranes for water purification and scalability and their health and environmental impacts: A review," *Nanomaterials*, vol. 12, no. 20, 2022, doi: 10.3390/nano12203637.

[13] M. R. Esfahani, S. A. Aktij, Z. Dabaghian, M. D. Firouzjaei, A. Rahimpour, J. Eke, I. C. Escobar, L. F. Greenlee, A.R. Esfahani, A. Sadmani, and N. Koutahzadeh, "Nanocomposite membranes for water separation and purification: Fabrication, modification, and applications," *Separation Purification Technology*, vol. 213, no. December 2018, pp. 465–499, 2019, doi: 10.1016/j.seppur.2018.12.050.

[14] J. H. Jhaveri and Z. V. P. Murthy, "Nanocomposite membranes," *Desalination and Water Treatment*, vol. 57, no. 55, pp. 26803–26819, 2016, doi: 10.1080/19443994.2015.1120687.

[15] A. Awasthi, P. Jadhao, and K. Kumari, "Clay nano-adsorbent: structures, applications and mechanism for water treatment," *SN Applied Science*, vol. 1, no. 9, pp. 1–21, 2019, doi: 10.1007/s42452-019-0858-9.

[16] A. Kausar, I. Ahmad, M. Maaza, and M. H. Eisa, "State-of-the-art nanoclay reinforcement in green polymeric nanocomposite: From design to new opportunities," *Minerals*, vol. 12, no. 12, pp. 1–23, 2022, doi: 10.3390/min12121495.

[17] I. C. E. Utari, U. Yanuhar, A. M. S. Hertika, H. Suryanto, J. Maulana, N.R. Caesar, M. Ismail, "Characterization and performance nanofiltration membranes in water quality for Goldfish (*Carassius auratus*) aquaculture," *Journal of Mechanical Engineering Science and Technology (JMEST)*, vol. 8, no. 2, pp. 332–344, Oct. 2024, doi: 10.17977/um016v8i22024p332.

[18] D. Shelly, V. Singhal, S. Singh, T. Nanda, R. Mehta, S.-Y. Lee, and S.-J. Park, "Exploring the Impact of Nanoclay on epoxy nanocomposites: A comprehensive review," *Journal of Composites Science*, vol. 8, no. 12, p. 506, 2024, doi: 10.3390/jcs8120506.

[19] T. Korumilli, A. Abdullahi, T. S. Kumar, and K. J. Rao, "22 - Nanoclay-reinforced bio-composites and their packaging applications," in *Nanoclay-Based Sustainable Materials*, V.V.T. Padil, Ed. Amsterdam, Netherlands : Elsevier, pp. 467–485, 2024, doi: 10.1016/B978-0-443-13390-9.00022-9.

[20] M. Muhajir, H. Suryanto, Y. R. A. Pradana, and U. Yanuhar, "Effect of homogenization pressure on bacterial cellulose membrane characteristic made from pineapple peel waste," *Journal of Mechanical Engineering Science and Technology (JMEST)*, vol. 6, no. 1, pp. 34–39, 2022, doi: 10.17977/um016v6i12022p034.

[21] N. K. Yadav, N. S. Rajput, S. Kulshreshtha, and M. K. Gupta, "Investigation of the mechanical and wear properties of epoxy resin composite (ERCs) made with nano particle TiO_2 and cotton fiber reinforcement," *Evergreen*, vol. 10, no. 1, pp. 63–77, 2023, doi: 10.5109/6781041.

[22] M. G. Ybañez and D. H. Camacho, "Designing hydrophobic bacterial cellulose film composites assisted by sound waves," *RSC Advanced*, vol. 11, no. 52, pp. 32873–32883, 2021, doi: 10.1039/d1ra02908h.

[23] ICDD Data Base, "Cellulose I beta," The International Centre for Diffraction Data, Ref. Code. 00-056-1718, 2012.

[24] R. Thandavamoorthy, Y. Devarajan, and S. Thanappan, "Analysis of the characterization of NaOH-treated natural cellulose fibre extracted from banyan aerial roots," *Scientific Report*, vol. 13, no. 1, p. 12579, 2023, doi: 10.1038/s41598-023-39229-9.

[25] W. Somphol, N. Chanka, and T. Boonmalert, "Extraction of cellulose nanocrystals and nanofibers from rubber leaves and their impacts on natural rubber properties," *Applied Science and Engineering Progress*, vol. 17, no. 2, 2024, Art.no. 7281, doi: 10.14416/j.asep.2023.11.010.

[26] P. Tsekova and O. Stoilova, "Fabrication of electrospun cellulose acetate/nanoclay composites for pollutant removal," *Polymers (Basel)*, vol. 14, no. 23, p. 5070, 2022, doi: 10.3390/polym14235070.

[27] G. Madhumitha, J. Fowsiya, S. Mohana Roopan, and V. K. Thakur, "Recent advances in starch–clay nanocomposites," *International Journal of Polymer Analysis and Characterization*, vol. 23, no. 4, pp. 331–345, May 2018, doi: 10.1080/1023666X.2018.1447260.

[28] N. Merah, F. Ashraf, and M. M. Shaukat, "Mechanical and moisture barrier properties of epoxy–nanoclay and hybrid epoxy–nanoclay glass fibre composites: A review," *Polymers (Basel)*, vol. 14, no. 8, p. 1640, 2022, doi: 10.3390/polym14081620.

[29] V. A. Agubra, P. S. Owuor, and M. V. Hosur, "Influence of nanoclay dispersion methods on the mechanical behavior of E-glass/epoxy nanocomposites," *Nanomaterials*, vol. 3, no. 3, pp. 550–563, 2013, doi: 10.3390/nano3030550.

[30] M. Razavi-Nouri, A. Sabet, M. Tayefi, and M. Imeni, "Effect of organoclay ordering and agglomeration on morphology and mechanical properties of uncured and dynamically cured ethylene-octene copolymer nanocomposites," *Macromolecular Materials and Engineering*, vol. 301, no. 12, pp. 1513–1524, Dec. 2016, doi: 10.1002/mame.201600255.

[31] R. Vârban, I. Crișan, D. Vârban, A. Ona, L. Olar, A. Stoie, and R. Ștefan, "Comparative FTIR prospecting for cellulose in stems of some fiber plants: Flax, velvet leaf, hemp and jute," *Applied Sciences*, vol. 11, no. 18, Sep. 2021, doi: 10.3390/app11188570.

[32] A. Bayraktar and C. Gürsoy, "Production of new nano-bacterial cellulose with *Lactobacillus rhamnosus* by using whey waste as substrate with optimization Tguchi method," *Research Square*, Jan. 05, 2024. doi: 10.21203/rs.3.rs-3828016/v1.

[33] M. Razavi-Nouri, A. Sabet, M. Tayefi, and M. Imeni, "Differentiating between natural and modified cellulosic fibres using ATR-FTIR spectroscopy," *Heritage*, vol. 5, no. 4, pp. 4114–4139, Dec. 2022, doi: 10.3390/heritage5040213.

[34] D. O. Govea-Alonso, M. J. García-Soto, L. Betancourt-Mendiola, E. Padilla-Ortega, S. Rosales-Mendoza, and O. González-Ortega, "Nanoclays: Promising materials for vaccinology," *Vaccines (Basel)*, vol. 10, no. 9, p. 1549, 2022, doi: 10.3390/vaccines10091549.

[35] F. N. Ajjan, M. J. Jafari, T. Rębiś, T. Ederth, and O. Inganäs, "Spectroelectrochemical investigation of redox states in a polypyrrole/lignin composite electrode material," *Journal of Materials Chemistry A*, vol. 3, no. 24,

pp. 12927–12937, Jun. 2015, doi: 10.1039/c5ta00788g.

[36] H. Farrokhi, M. Koosha, N. Nasirizadeh, M. Salari, M. Abdouss, T. Li, and Y. Gong, "The effect of nanoclay type on the mechanical properties and antibacterial activity of Chitosan/PVA nanocomposite films," *Journal of Composites Science*, vol. 8, no. 7, Jul. 2024, doi: 10.3390/jcs8070255.

[37] J. J. Encalada-Alayola, Y. Veranes-Pantoja, J. A. Uribe-Calderón, J. V. Cauich-Rodríguez, and J. M. Cervantes-Uc, "Effect of type and concentration of nanoclay on the mechanical and physicochemical properties of bis-GMA/TTEGDMA dental resins," *Polymers (Basel)*, vol. 12, no. 3, Mar. 2020, doi: 10.3390/polym12030601.

[38] H. Y. Ünal, G. Öner, and Y. Pekbey, "Comparison of the experimental mechanical properties and DMA measurement of nanoclay hybrid composites," *European Mechanical Science*, vol. 2, no. 1, pp. 31–36, Dec. 2017, doi: 10.26701/ems.356823.

[39] Y. Zare and K. Y. Rhee, "Simulation of Young's modulus for clay-reinforced nanocomposites assuming mechanical percolation, clay-interphase networks and interfacial linkage," *Journal of Materials Research and Technology*, vol. 9, no. 6, pp. 12473–12483, Nov. 2020, doi: 10.1016/j.jmrt.2020.08.097.

[40] A. Ahmed, A. A. Mahmoud, and S. Elkatatny, "The combined effect of nanoclay powder and curing time on the properties of class G cement," *Geofluids*, vol. 2023, 2023, doi: 10.1155/2023/7316335.

[41] T. R. Sobahi, M. Y. Abdelaal, and M. A. Salam, "Structure and physical properties of cellulose triacetate/nanoclay nanocomposites," *Indian Journal of Chemical Technology*, vol. 27, pp. 85–89, 2020.

[42] M. H. Gabr, N. T. Phong, M. A. Abdelkareem, K. Okubo, K. Uzawa, I. Kimpara, and T. Fujii, "Mechanical, thermal, and moisture absorption properties of nano-clay reinforced nano-cellulose biocomposites," *Cellulose*, vol. 20, no. 2, pp. 819–826, 2013, doi: 10.1007/s10570-013-9876-8.

[43] S. S. Chee, M. Jawaid, O. Y. Alothman, and H. Fouad, "Effects of nanoclay on mechanical and dynamic mechanical properties of bamboo/kenaf reinforced epoxy hybrid composites," *Polymers (Basel)*, vol. 13, no. 3, 2021, doi: 10.3390/polym13030395.

[44] S. I. Hossain, E. A. Kukushkina, M. Izzi, M. C. Sportelli, R. A. Picca, N. Ditaranto, and N. Cioffi, "A Review on Montmorillonite-Based Nanoantimicrobials: State of the Art," *Nanomaterials*, vol. 13, no. 5, p. 848, 2023, doi: 10.3390/nano13050848.

[45] M. Z. M. Vazifeh, S. M. Hosseini, M. H. Seyed, A. Mohammadi, and H. Maleki, "Investigation of the antimicrobial properties of nanoclay and chitosan based nanocomposite on the microbial characteristics of Gouda cheese," *Iranian Journal of Microbiology*, vol. 12, no. 2, pp. 121–126, 2020.

[46] A. H. Mohsen, N. A. Ali, S. I. Hussein, A. Y. A. Mohammed, A. M. Alraih, and A. M. Abd-Elnaiem, "Investigation of optical, mechanical, thermal, wettability, and antibacterial activity of polyvinyl alcohol mixed with clay nanoparticles," *Inorganic Chemistry Communication*, vol. 167, 2024, Art. no. 112841, doi: 10.1016/j.inoche.2024.112841.

[47] M. Lee, D. Kim, J. Kim, J. K. Oh, H. Castaneda, and J. H. Kim, "Antimicrobial Activities of Thermoplastic polyurethane/clay nano-composites against pathogenic bacteria," *ACS Applied Bio Materials*, vol. 3, no. 10, pp. 6672–6679, Oct. 2020, doi: 10.1021/acsabm.0c00452.

[48] J. Ren, H. Weng, B. Li, F. Chen, J. Liu, and Z. Song, "The influence mechanism of pore structure of tectonically deformed coal on the adsorption and desorption hysteresis," *Frontier Earth Science*, vol. 10, 2022, doi: 10.3389/feart.2022.841353.

[49] I. A. Borojeni, A. Jenab, M. Sanjari, and C. Boudreault, "Effect of nanoclay addition on the morphology, fiber size distribution and pore size of electrospun polyvinylpyrrolidone (PVP) composite fibers for air filter applications," *Fibers*, vol. 9, no. 8, 2021, doi: 10.3390/fib9080048.